



HAL
open science

Nuclear profiles of H3 histones trimethylated on Lys27 in bovine (*Bos Taurus*) embryos obtained after in vitro fertilization or somatic cell nuclear transfer

Amandine Breton, Daniel D. Le Bourhis, Christophe C. Audouard, Xavier Vignon, Jean-Marc J.-M. Lelievre

► To cite this version:

Amandine Breton, Daniel D. Le Bourhis, Christophe C. Audouard, Xavier Vignon, Jean-Marc J.-M. Lelievre. Nuclear profiles of H3 histones trimethylated on Lys27 in bovine (*Bos Taurus*) embryos obtained after in vitro fertilization or somatic cell nuclear transfer. *Journal of Reproduction and Development*, 2010, 56 (4), pp.379-388. 10.1262/jrd.09-182A . hal-02668059

HAL Id: hal-02668059

<https://hal.inrae.fr/hal-02668059>

Submitted on 31 May 2020

HAL is a multi-disciplinary open access archive for the deposit and dissemination of scientific research documents, whether they are published or not. The documents may come from teaching and research institutions in France or abroad, or from public or private research centers.

L'archive ouverte pluridisciplinaire **HAL**, est destinée au dépôt et à la diffusion de documents scientifiques de niveau recherche, publiés ou non, émanant des établissements d'enseignement et de recherche français ou étrangers, des laboratoires publics ou privés.



Distributed under a Creative Commons Attribution - ShareAlike 4.0 International License

—Original Article—

Nuclear Profiles of H3 Histones Trimethylated on Lys27 in Bovine (*Bos taurus*) Embryos Obtained after *In Vitro* Fertilization or Somatic Cell Nuclear Transfer

Amandine BRETON¹⁾, Daniel LE BOURHIS^{1,2)}, Christophe AUDOUARD^{1)#},
Xavier VIGNON¹⁾ and Jean-Marc LELIÈVRE¹⁾

¹⁾INRA, ENVA UMR 1198 Biologie du Développement et Reproduction, F-78350 Jouy en Josas and ²⁾UNCEIA, Département R&D, F-94704 Maison-Alfort, France

#Present: Centre de Biologie du Développement, Université Paul Sabatier 118, F-31062 Toulouse, France

Abstract. Histone H3 trimethylation on lysine 27 is one of the histone modifications associated with chromatin of silenced regions. H3K27me3 labeling is initially asymmetrical between pronuclei in mammalian embryos, and then it is remodeled during early development. However, in mouse embryos obtained after somatic cell nuclear transfer (SCNT), H3K27me3 histones inherited from the somatic female cell and associated with X chromosome inactivation have been reported to escape remodeling. Using immunostaining, we investigated the remodeling of H3K27me3 in *Bos taurus* embryos obtained after *in vitro* fertilization (IVF) and SCNT. In this species, transfer-induced chromatin remodeling can be clearly separated from embryonic genome activation (EGA), which occurs at the 8–16-cell stage, and cloning by SCNT is 10 times more successful than in the mouse. In early IVF bovine embryos, dense H3K27me3 labeling was localized in the pericentric heterochromatin as recently described in the mouse. Labeling was however unevenly distributed up to the 8-cell stage, suggesting that the parental genomes partitioned before EGA. In female IVF blastocysts, a somatic-like female profile appeared in 21% of the trophoblast cells. This profile, which had one major nuclear H3K27me3 patch, the putative inactive X chromosome (Xi), was absent in male blastocysts. In contrast, the somatic-like female H3K27me3 profile was observed in the majority of the nuclei of female bovine SCNT embryos before EGA. At the 8–16-cell stage, this profile was transiently replaced by pericentric-like labeling in most nuclei. Immunostaining of mitotic chromosomes suggested that the ratio of H3K27me3 labeling in pericentric heterochromatin vs. euchromatin was then rapidly altered. Finally, Xi-like H3K27me3 staining appeared again in trophoblast cells in female SCNT blastocysts. These results suggest a role for EGA in H3K27me3 remodeling, which affects the heterochromatin inherited from the donor cell or produced during development.

Key words: Heterochromatin, Preimplantation embryo, Somatic cloning

(J. Reprod. Dev. 56: 379–388, 2010)

The low developmental potential of embryos obtained after somatic cell nuclear transfer (SCNT) into oocyte cytoplasm suggests that the transformation of nuclei of differentiated cells into a fully totipotent state in the early SCNT embryo is inefficient [1]. One of the hypotheses to explain this faulty ‘reprogramming’ points to the different nuclear factors that make up the environment surrounding the DNA and that are transmitted by the donor cell, i.e., epigenetic factors [2, 3]. Epigenetic nuclear factors include methylation of the DNA, nucleosome structure and association of non-histone proteins. In nucleosomes, covalent histone modifications have emerged as a key mechanism that is very closely linked to transcriptional regulation [46]. In the case of SCNT, the nucleus of the donor cell carries its own epigenetic structures, which are different from the ones carried by the gametes, and may prevent or modify acquisition of the epigenetic structures associated with normal embryogenesis. Epigenetic nuclear events that normally take place during embryogenesis have indeed been found to be abnor-

mal or incomplete—sometimes in relation with altered gene expression [7]—in SCNT embryos and organisms (reviewed by [1, 3, 8]). This may give rise to developmental anomalies and early death, which are frequently observed in mammalian clones [9, 10] (reviewed by [1, 11]).

Here, we have focused on one N-terminal covalent histone modification that is particularly present in heterochromatin and other transcriptionally silent genomic regions, the trimethylation of histone H3 on lysine 27 (H3K27me3). This allowed us to investigate the remodeling of the facultative heterochromatin formed by the transcriptionally inactive X (Xi) chromosome inherited from the somatic female donor nucleus and to compare the dynamics of the nuclear events associated with H3K27me3 in bovine embryos obtained after *in vitro* fertilization (IVF) and SCNT. In early mouse embryos, H3K27me3 is successively accumulated in the paternally inherited pericentric regions forming constitutive heterochromatin and the inactive X (Xi) chromosome of female cells forming facultative heterochromatin [12]. Although numerous other regions (in euchromatin) are enriched in H3K27me3 [13, 14], pericentric and Xi-associated heterochromatin forms condensed territories in the nucleus, such as chromocenters for constitutive heterochromatin [15] and the Barr body for the X chromosome

Received: October 19, 2009

Accepted: March 15, 2010

Published online in J-STAGE: April 22, 2010

©2010 by the Society for Reproduction and Development

Correspondence: J-M Lelièvre (e-mail: jean-marc.lelievre@jouy.inra.fr)

[16].

H3K27me3 formation is catalyzed by a multiprotein complex called the Polycomb repressor complex PRC2 [17]. Subsequently, H3K27me3 facilitates the loading of PRC1, which mediates transcriptional silencing per se, although PRC2-independent recruitment of PRC1 can also occur [12, 18, 19]. In early mouse embryos, paternally inherited pericentric regions form heterochromatin that is transiently enriched in histone H3K27me3, PRC1 and PRC2 after fertilization. In contrast, their maternally inherited counterparts are silenced via the same dominant pathway that prevails in somatic cells, namely trimethylation of histone H3 on lysine 9 (H3K9me3) by the Suv39h histone methyltransferases during oogenesis [12]. Histone H3K9me3 and heterochromatin protein HP1 progressively replace histone H3K27me3 in the paternal pericentric heterochromatin, giving rise to H3K9me3 and HP1 in all the pericentric heterochromatin at the morula stage [12]. This situation, which is also found in the constitutive heterochromatin of embryonic stem cells and somatic cells, suggests a hierarchy between PRC2-mediated and Suv39h-mediated silencing [20]. Simultaneously, the nuclear localization of centromeres and pericentric regions undergoes profound reorganization during and immediately after embryonic genome activation (EGA), leading to the formation of chromocenters [15]. This spatial reorganization may take place properly at the same development stage, at least in a proportion of NT mouse embryos [21, 22].

At the blastocyst stage, Xi-associated histone H3K27me3 becomes particularly visible as a large patch in the nuclei of female mouse embryos [23, 24]. Although H3K27me3 enrichment is not sufficient to infer gene silencing at this stage [25], it is clearly necessary to X chromosome inactivation (XCI) in placental tissues [26, 27]. H3K27me3 enrichment coincides with the initial implementation of XCI at the blastocyst stage, i.e., one of the X chromosomes transcriptionally silenced. The inactivated X-specific transcript *Xist* RNA, which triggers XCI and is detected from the 2–4-cell stage on the paternally-inherited X^P chromosome, starts to accumulate on the X^P chromosome from the morula/blastocyst stages in female mouse embryos ([28] and reviewed in [16]).

In female mouse SCNT embryos, immunostaining has shown, however, that one H3K27me3-rich, X-associated patch is present from the one-cell stage up to the blastocyst stage in most cells of mouse SCNT embryos [28]. This suggests that the H3K27me3 patch is most likely associated with the Xi inherited from the female donor cell and may correspond to the absence of remodeling of the H3K27me3-rich regions [28] that are present on the Xi of somatic female cells [29]. This is associated with the delayed and often abnormal expression pattern of *Xist* RNA, since it is detected after the 8-cell stage only and is biallelically expressed in mouse SCNT embryos [28, 30]. Taken together, these data suggest that H3K27me3 may provide a valuable marker for comparing chromatin at the nuclear level in normal and SCNT embryos.

The success rate of bovine cloning by SCNT is close to 10% or even higher, while mouse SCNT efficiency reaches only 1–2% [1], making bovine embryos a material of choice for studying the events that follow nuclear transfer. Moreover, the early bovine embryo displays features that differ significantly from the mouse embryo. Among them is the transition phase from maternal control

to embryonic control of development. This phase is longer in bovine than in mouse embryos since the EGA necessary for continuation of development occurs at the 8–16-cell stage in the former and at the two-cell stage in the latter (reviewed by [31, 32]). Consequently, nuclear transfer induced remodeling and early embryonic genome transcription are clearly separate stages in bovine SCNT embryos. Finally, the formation of bovine blastocysts is also delayed by one or two cell cycles. In contrast, the XCI pattern described in the mouse seems to be largely conserved in cultured bovine embryos, where it also takes place at the blastocyst stage [33]. The organization of constitutive heterochromatin is also conserved in bovine and mouse somatic cells; during interphase, centromeres and pericentric regions of several chromosomes aggregate to form chromocenters, and in both cases, this organization is acquired from the EGA stage onwards [15, 34].

Most epigenetic studies have addressed the remodeling of DNA methylation in bovine SCNT embryos [35, 38]. Abnormal methylation patterns have been reported in tissues of abnormal and deceased bovine clones [38] and may be associated with the aberrant expression of imprinted and non-imprinted genes that has been observed in deceased SCNT newborn calves [39, 42]. Remodeling of DNA methylation and of one covalent histone modification has been shown to correlate with developmental potential in early embryos obtained after nuclear transfer of different types of donor cells [43]. In our study, we investigated first the intranuclear localization of trimethylated H3K27 in IVF bovine embryos and then compared it with its remodeling in embryos obtained after SCNT. Moreover, since it has been shown that H3K27me3 is involved in the process of X inactivation, the remodeling pattern of this epigenetic mark was analyzed according to the sex of the embryos.

Methods

Bovine fibroblasts

Female 5538 and male OV7060 bovine fibroblast cultures were derived from adult skin biopsies. Cultures were made in plastic Petri dishes in Dulbecco's Modified Eagle Medium (DMEM) supplemented with 10% fetal calf serum (FCS) and antibiotics. Confluent cells were recovered after trypsin treatment and diluted 3 times in DMEM before plating or frozen after being resuspended in concentrated FCS. Each trypsin treatment increases the number of 'passages' the culture undergoes. For immunofluorescence, cells were plated on SuperFrost slides. For SCNT and immunofluorescence, confluent fibroblasts were kept for another four days before nuclear transfer in fresh DMEM medium supplemented with 10% FCS. Donor cells were used from passage 4 to passage 10. The cells exhibited a normal karyotype in more than 70% of the metaphases observed. Furthermore, all the SCNT embryos generated in our laboratory with the 5538 cells routinely yielded a high percentage of viable offspring; around 20% of the blastocysts obtained after 5538 SCNT ('genotype A' in [44]) and transferred into recipient heifers developed to term [44].

In vitro oocyte maturation, fertilization and somatic cell nuclear transfer

All procedures have been described previously [45]. The same

Table 1. Evolution of the H3K27me3 histone pattern during early development of cultured female bovine embryos obtained after IVF or SCNT

Group	Developmental stage	Time (hours post-insemination or -fusion)	Number of embryos	Number of (pro)nuclei / total number of (pro)nuclei (%) showing one of the two main H3K27me3 labeling patterns	
				Type 1 labeling ^a	Type 2 labeling ^a
<i>In vitro</i> fertilization	Zygote 2PN	16–18 hpi	9	0/18 (0)	0/18 (0)
	2–4 cells	30–32	10	0/24 (0)	0/24 (0)
	4–8 cells	44–48	15	9/110 (8)	0/110 (0)
	8–16 cells	68–74	12	145/134 (97)	0/134 (0)
	16–32 cells	94–100	10	192/207 (93)	0/207 (0)
	Morula	115–120	23	681/740 (92)	3/740 (0)
	Blastocyst ^b	170–190	11	nd	250/1177 (21) ^c
Somatic cell nuclear transfer	1 cell	16–18 hpf	15	0/15 (0)	8/15 (54)
	2 cells	25–28	20	0/40 (0)	20/40 (50)
	4–8 cells	40–44	12	19/82 (23)	56/82 (68)
	8–16 cells	68–74	12	92/107 (86)	11/107 (9)
	16–32 cells	94–100	14	194/285 (68)	14/285 (4)
	Morula	115–120	20	382/621 (62)	36/621 (6)
	Blastocyst	170–190	29	nd	675/2469 (27) ^c

^a Type 1, 'pericentric labeling' (IVF) or 'pericentric-like labeling' (SCNT), corresponds to dense labeling of pericentric dots and low labeling signal in the euchromatin; type 2, 'somatic-like female labeling', corresponds to one large patch, the putative Xi. ^b Putative IVF female embryos, i.e., containing at least 5 nuclei with the H3K27me3 somatic-like female pattern. ^c The percentage is given in consideration of immunostained nuclei only, which excluded nuclei of the inner cell mass and included $\geq 90\%$ of the nuclei of the trophoblast cells in our conditions.

batches of matured oocytes were used for IVF and SCNT. Sixty to 80% of matured oocytes cleaved after incubation with high-quality semen. The rate of IVF blastocysts was on average 35%. Cleavage and blastocyst rates for female SCNT embryos were on average 85 and 55%, respectively, and on average 85 and 66% for male SCNT embryos.

In vitro embryo culture

After IVF or SCNT, presumptive zygotes or reconstituted embryos were cultured in microdrops of 50 μ l B2 medium (Laboratoire C.C.D., Paris, France) [46] with 2.5% FCS, seeded with Vero cells [45]. The droplets were overlaid with mineral oil and incubated at 39 C under 5% CO₂ conditions. Cleavage was assessed at day 1 post-insemination or post-fusion, and blastocyst formation was evaluated at day 7. Embryos were harvested at different developmental stages as described in Table 1.

Preparation of fibroblasts for immunostaining

Cells grown on slides were pre-permeabilized in cold phosphate buffered saline (PBS) supplemented with 0.2% Triton X-100 for 7 min prior to fixation in 4% paraformaldehyde in PBS for 15 min at room temperature. After three washes in PBS, the cells were post-permeabilized in PBS-0.5% Triton X-100 at room temperature for 10–15 min.

Preparation of bovine embryos for immunostaining

All embryos were collected and placed in PBS before fixation or removal of the zona pellucida with Pronase (Ref P5147 from Sigma, St. Quentin Fallavier, France) at 37 C for 5 min. After the Pronase activity had been inhibited in B2 medium supplemented with 2.5% FCS, embryos at the morula and blastocyst stages were pre-permeabilized in PBS-0.2% Triton X-100 on ice for 5 min and

washed in PBS-0.5% bovine serum albumin. At earlier stages, this step was omitted, and embryos were fixed directly in 4% paraformaldehyde or after removal of the zona pellucida. All embryos were post-permeabilized by 0.5% Triton X-100 treatment for 15 min to 30 min, depending on the stages and presence or absence of the zona pellucida. For blastocyst embryos, our experimental procedure was only optimized for the analysis of trophoblastic cells. Under these conditions, cells of the inner cell mass were insufficiently permeabilized to highlight specific H3K27me3 signals in their nuclei and were not taken into account.

Indirect immunofluorescence

After the blocking step in 2% bovine serum albumin - 0.05% Triton X100 - 0.05% Tween - PBS, cells and embryos were sequentially incubated overnight at 4 C with primary antibodies, then for 1 h at room temperature with secondary antibodies. Between the two antibody reactions, cells and embryos were washed in 0.05% Tween - PBS and again blocked for 15 min. All antibodies were diluted in the blocking solution. Commercial anti-H3K27me3 antibodies (Upstate 07-449) were diluted 500 times for immunostaining. Anti-H3K9me3 (Abcam ab8898) antibodies were diluted 300 times. Anti-rabbit IgG coupled to FITC (Jackson 211-095-109), anti-rabbit IgG coupled to TRITC (Jackson 211-025-109), anti-sheep IgG coupled to FITC (Jackson 713-095-147) and anti-sheep IgG coupled to TRITC (Jackson 715-025-147) antibodies were diluted 200 times. Anti-digoxigenin (Roche 11 333 08) antibodies were used as a 400-fold dilution. Finally, cells and embryos were rinsed in 0.05% Tween - PBS before being counterstained and mounted in Vectashield (Vector Laboratories, Burlingame, USA). For DNA counterstaining, 1 μ g.ml⁻¹ Hoechst 33342 (Sigma-Aldrich) and 3.3 μ g.ml⁻¹ YOYO-1 (Invitrogen, Cergy Pontoise, France) were used for epifluorescence and confo-

cal microscopy observation, respectively.

Microscopy and image analysis

Fibroblast cells were observed using digital imaging microscopy with an epifluorescence microscope Axiovert (Zeiss, Le Pecq, France) and $\times 40$ and $\times 100$ oil immersion objectives (numerical aperture=1.3). Fibroblast images were recorded digitally with a high resolution CCD camera using IPLab image analysis software. In some cases, grayscale images were pseudo-colored after capture using Image J. Digital optical sections from IVF and SCNT preimplantation embryos were recorded using a confocal laser scanning microscope (Zeiss LSM 510) with an $\times 63$ oil immersion objective (numerical aperture=1.4). For the figures, depending on the stage, complete or partial projections of the confocal images were generated using the Z project plug-in of the *ImageJ* software (http://rsb.info.nih.gov/ij/java1.5.0_13) based on the maximum intensity. Cells were counted after projection of all stacks. All nuclei were numbered according to the H3K27me3 patterns in embryos at early stages, from 1 to 32 cells. At morula and blastocyst stage, 0 to 5% and 0 to 10% of the nuclei were not immunostained, respectively, and were not recorded. At the blastocyst stage, only trophectodermal nuclei were analyzed as mentioned above.

Results and Discussion

Analysis of H3K27me3-rich nuclear regions during development in IVF bovine embryos

Using commercial antibodies directed against the peptide motif of branched trimethylated lysines 27 on histones H3 (H3K27me3), the nuclear profiles in bovine embryos were analyzed up to the blastocyst stage. In zygotes, H3K27me3 immunolabeling was observed in one of the pronuclei and in the polar bodies (Fig. 1). This labeling appeared as a few dense spots surrounded by a homogeneous signal in the nucleoplasm. This corroborates the data of Ross *et al.* [47], who showed unambiguously that only the female pronucleus is enriched with H3K27me3 histones in bovine embryos. At the 2-cell stage and up to the early 8-cell stage, the H3K27me3 labeling was unevenly distributed in most nuclei (Fig. 2a). Intense spots appeared clearly and randomly distributed in most nuclei at late 8–16-cell (not shown), early 16–32-cell (Fig. 2a) and morula (Fig. 3a) stages and in a proportion of the nuclei from blastocyst embryos (Fig. 3b). The evolution of this pattern seems to support the global decrease in H3K27me3 labeling signals following fertilization reported by Ross *et al.* [47] in bovine embryos. Since this pattern was found in more than 90% of embryos, it had no relationship with the sex chromosome content.

On several occasions, we were able to observe H3K27me3 immunolabeling directly on mitotic chromosomes in 16–32-cell embryos. H3K27me3 spots were clearly seen on the ends of 20 to 30 chromosomes (Fig. 2b). Given that all bovine autosomes are acrocentric, the polarization of the labeling strongly suggests that H3K27me3 spots were close to the centromeres (Fig. 2b, M), namely in the pericentric regions as demonstrated in the mouse [12, 48]. This profile will therefore be referred to as the pericentric profile.

In bovine IVF embryos, crescent shaped H3K27me3 immun-

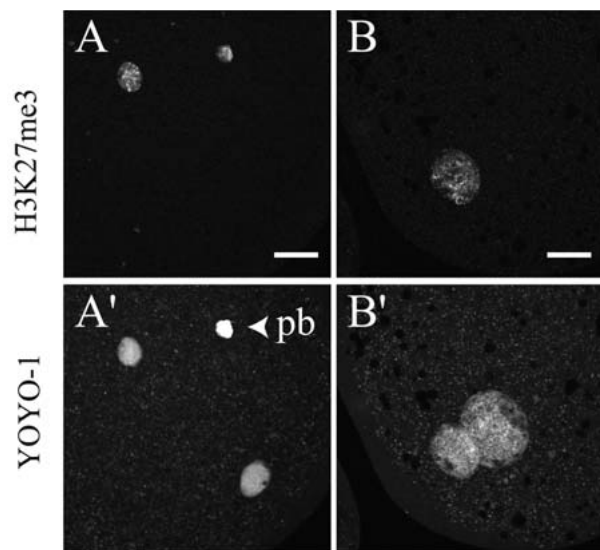


Fig. 1. Differential H3K27me3 immunostaining in zygotes at the pronuclei stage. Matured oocytes were harvested 16 to 18 h post insemination, fixed and permeabilized before immunostaining. Antibodies against H3 histones trimethylated on lysine 27 (H3K27me3) were used to immunolocalize the modified histones in the two pronuclei. Nuclear DNA was counterstained with YOYO-1. In the late embryo (A), H3K27me3 is strongly detected in the polar body and the closest pronucleus. The H3K27me3-free pronucleus is moderately enlarged. In the more advanced embryo (B), the H3K27me3-free pronucleus has enlarged and moved closer to the positively immunostained pronucleus. Scale bars: 20 μ m.

ostaining was encountered at the 2-cell and 4–8-cell stages (Fig. 2a), i.e., up to the beginning of EGA. Cowell *et al.* [49] have also observed uneven nuclear labeling with H3K9me3 in early mouse embryos before and during EGA, at the 1- and 2–4-cell stages. It has been postulated that uneven labeling is the consequence of asymmetrical labeling between the paternal and maternal chromosomes in their pronuclei [49]. In mouse embryos, it is well established that at the 2-cell stage the two genomes remain partitioned in the interphase nucleus [50]. Since H3K9me3 labeling is detected in the maternal pronucleus only, this leads to asymmetrical labeling of the two parental genomes at the two-cell stage [49]. We also observed in bovine embryos an asymmetrical labeling in the nuclei up to the late 8–16-cell stage (Fig. 2a), probably because the parental genomes remain partitioned until this stage. Therefore, in both mouse [49, 50] and bovine (this paper) embryos, partitioning of the parental genomes disappears after EGA, strongly suggesting a link between partition of the parental genomes and genome-wide transcription.

The asymmetry for PRC2-associated H3K27me3 between pronuclei -namely the high level in the female pronucleus- has been demonstrated in mouse ([12, 48] and references therein), bovine ([47], this paper) and pig [51] embryos. However, in mouse embryos, H3K27me3 immunolabeling is observed in the pericentric regions in the late male pronucleus; transient enrichment in

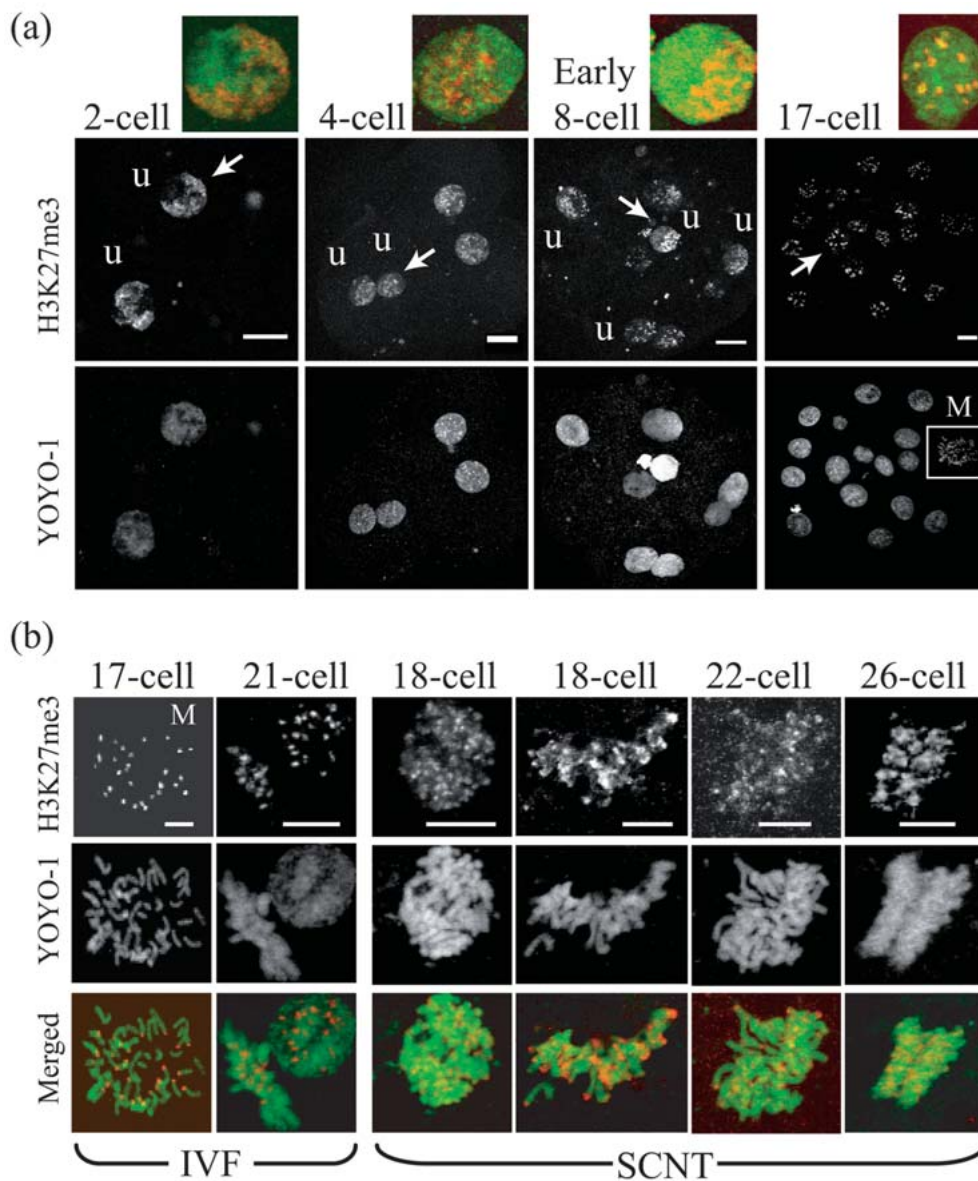


Fig. 2. Enrichment in H3K27me3 of pericentric heterochromatin in early bovine embryos. Cultured embryos were harvested at the appropriate stages and immunostained as described in Fig. 1. (a) The embryos obtained after *in vitro* fertilization (IVF) and recovered before embryonic genome activation (EGA) at the 2-cell, 4-cell, early 8-cell stages or after EGA (17-cell stage) were fixed in 4% formaldehyde and then permeabilized. Arrows indicate the magnified nuclei; nuclei showing an uneven distribution of labeled H3K27me3 histones are indicated by letter u. (b) Magnifications of H3K27me3 and DNA profiles of metaphases of IVF (left panel) and SCNT (right panel) 16–32-cell embryos. The metaphase M of the 17-cell IVF embryo originates from the 17-cell embryo shown in a. In the color prints, immunolabeling is in red and YOYO-1 in green. H3K27me3 spots are located on one extremity of many chromosomes as seen on the merged image, strongly suggesting that the spots observed in (interphase) nuclei are localized in pericentric regions. GC-rich bovine centromeres and pericentromeres are poorly stained by YOYO-1. Scale bars: (a) 20 μm ; (b) 10 μm .

H3K27me3 of other non-pericentric regions is observed in the female pronucleus but disappears during the 2nd cell cycle [12]. In bovine embryos at the late pronucleus stage (Fig. 1B, B'), H3K27me3 was not detected when the male pronucleus was greatly enlarged and close to the female pronucleus. Altogether, these data strongly suggest that in bovine embryos H3K27me3 is initially enriched on the chromatin inherited from the mother and becomes

transiently restricted to the pericentric regions during EGA; it remains to be determined whether this latter localization depends on the parental origin in bovine embryos or not.

In 39% (11/28) of the IVF embryos analyzed at the blastocyst stage, on average 21% of the trophoblast cells displayed one large H3K27me3 peripheral signal in the nuclei (Fig. 3b), suggesting the presence of the Xi-associated H3K27me3 patch as observed in

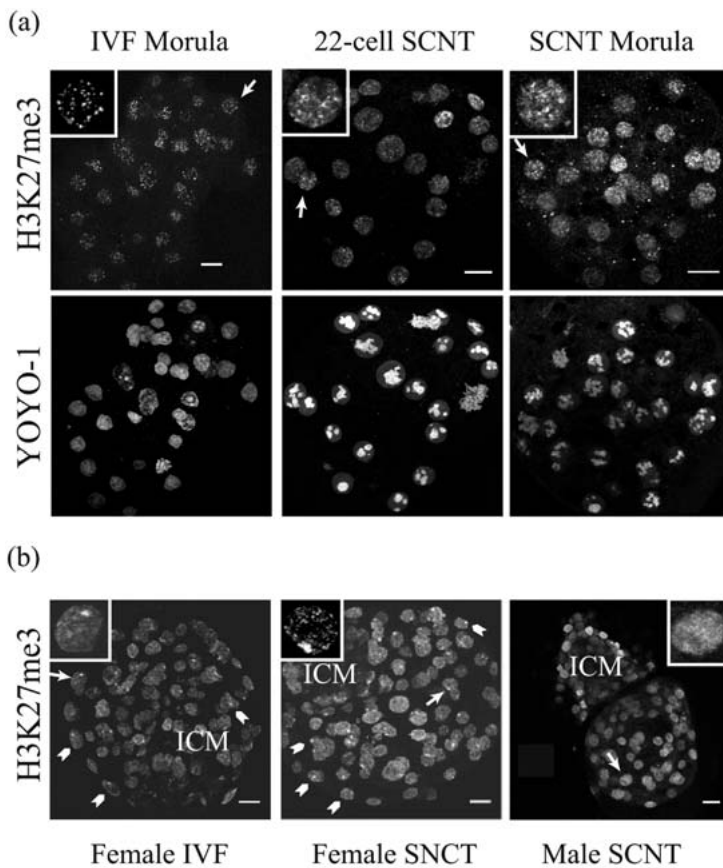


Fig. 3. The evolution of H3K27me3 nuclear profiles in bovine embryos after embryo genome activation. Immunostaining was performed as described in Fig. 1 except that morula and blastocyst embryos were permeabilized before and after fixation to reduce non-specific signals and ensure proper access to the epitopes. The multi-dot, pericentric H3K27me3 profile described in Fig. 2 disappeared between the morula (a) and blastocyst (b) stages in both IVF and SCNT embryos. (a) At the 16–32-cell and morula stages, a pericentric-like profile was found in the majority of the nuclei of 90% of the female SCNT embryos, but it was more heterogeneous than in those of the IVF embryos. (b) At the blastocyst stage, on average 21 and 27% of the nuclei of the trophoblast cells in the female IVF and SCNT embryos displayed the somatic-like female profile, respectively (arrowheads), suggesting that an X-associated H3K27me3-rich patch was present in these cells. This profile was absent in the male IVF and SCNT embryos. Arrows indicate the magnified nuclei. Scale bars: 20 μ m.

somatic female cells ([23, 24] and see below). This concurs with what is known from the XCI process, which is detected at least in some cells in female bovine IVF embryos at the blastocyst stage [33]. In a specific experiment, biopsies were recovered from embryos (N=10) before fixation to sex them using PCR as previously described [52, 53]. After immunolabeling of the sexed embryos, the Xi-like H3K27me3 patch was detected exclusively in female embryos (data not shown).

To test if our immunostaining procedures were compatible with antigen access in bovine embryos between the key 8-cell and blastocyst stages, immunolabeling was performed under the same conditions with antibodies directed against H3K9me3. H3K9me3 labeling displayed the expected profile, since it was concentrated in several spots from the 8–16-cell stage to the blastocyst stage (data not shown). Therefore, the H3K9me3 pattern in the blastocysts conformed to the well-established preferential H3K9me3 labeling of pericentric regions in somatic and embryonic cells after EGA ([12] and references therein). This result confirmed that in our immunostaining conditions, the low frequency of Xi-like H3K27me3 patches and the decrease in H3K27me3 labeling in pericentromeric heterochromatin were not the result of a lack of antigen accessibility or of a simple change in chromatin compaction [54].

H3K27me3 nuclear profiles of female and male bovine fibroblasts

The H3K27me3 nuclear profiles in bovine fibroblast cells were analyzed (Fig. 4a). The bovine Xi chromosome displays two intense H3K27me3-rich bands at metaphase [55]. During interphase, a bright, heavily labeled patch was visible in the nucleus (Fig. 4a) of a proportion of female fibroblast cells varying from 30 to 70% as reported by others in the mouse [28]. This profile was never observed in male fibroblast cells (data not shown). The fate of this H3K27me3-rich nuclear region was then studied after nuclear transfer of the bovine fibroblast nuclei into enucleated bovine oocytes.

Analysis of H3K27me3-rich nuclear regions during development in female and male SCNT embryos

Previous studies have revealed that clones of lower potential displayed hypermethylation of DNA and H3K9 as compared with IVF embryos [43]. These hypermethylated regions had not been identified but most likely correspond to pericentric heterochromatin [43] as shown by another study [35]. Here, we focused on H3K27me3 (Table 1).

On average, 85% of 1-cell SCNT embryos cleaved, and 65% reached the 4–8-cell stage. The 8–16-cell embryos represented on average 55% of the reconstituted embryos, i.e., 85% of the 4–8-cell

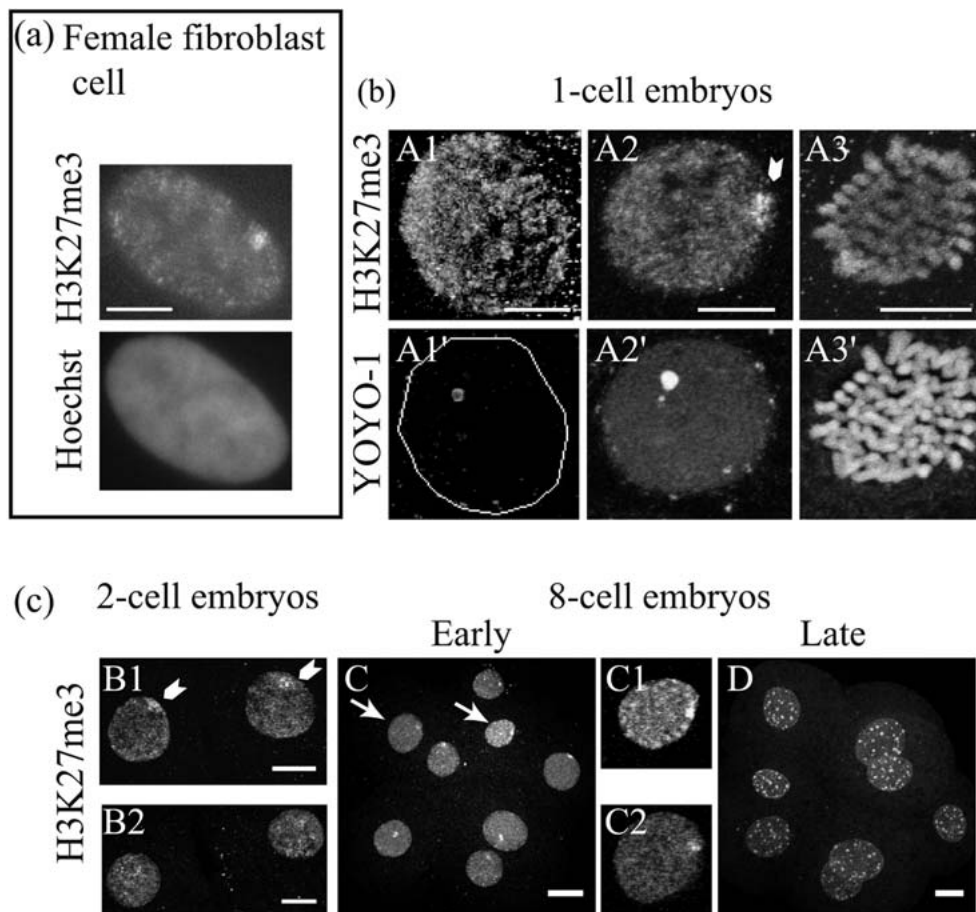


Fig. 4. Representative H3K27me3 nuclear profiles in female bovine SCNT embryos up to embryo genome activation. H3K27me3 immunostaining in female SCNT embryos and donor (fibroblast) cells was performed as in Fig. 1 and Fig. 3, respectively. Embryos were fixed (b) at the one-cell stage at 16–18 hpf (A1 & A2), (c) at the 2-cell stage at 27 hpf (B1 & B2) and at the early (46 hpf, C, C1 & C2) and late (70 hpf, D) 8-cell stages. DNA was stained with YOYO-1. Arrowheads indicate nuclei with the putative Xi-associated patch. The magnified views correspond to the nuclei indicated by the arrows. Scale bars: (a) 2 μm ; (b) 10 μm ; (c) 20 μm .

embryo population and 65% of the cleaved embryos. More than 95% of the 8–16-cell embryos reached the blastocyst stage.

Sixty-five percent (15/23) of the female bovine 1-cell SCNT embryos fixed at 16–18 h post-fusion (hpf) displayed expanded nuclei, and in two embryos the nuclei were in metaphase. In 26% (6/23) of the observed embryos, poorly expanded nuclei were seen; these embryos were most likely blocked and were not considered for H3K27me3 analysis. About half (8/15) of the expanded nuclei displayed the nuclear H3K27me3 profile close to the one observed in IVF embryos at this stage, except that immunostaining was observed throughout the nucleus (Fig. 4b, A1). The remaining half displayed a somatic-like female profile characterized by an H3K27me3 patch (Table 1, Fig. 4a, A2). Since such a pattern was not observed in IVF embryos at this stage, this suggests that in a proportion of SCNT embryos, the Xi chromosomal territory remained the main heterochromatin region enriched by these modified histones during chromatin remodeling. Metaphase figures

indicate that H3K27me3 was present along the whole chromosomes at the end of the first cycle (Fig. 4b, A3).

At the 2-cell stage, an Xi-like H3K27me3 patch was detected in both nuclei of 50% of the embryos (Table 1), although it was not as clearly delineated as in the somatic nucleus (Fig. 4c, B1). In the remaining embryos, the patterns were similar to those observed in IVF embryos, except that labeling was found throughout the whole nucleus (Fig. 4c, B2) as expected in the absence of parental based genome partition. In the 4–8-cell embryos, a dominant peripheral patch with or without numerous smaller dots was found. These patterns that were both considered to be somatic-like female profiles were found in 68% of the nuclei (Table 1; Fig. 4c, C) and 75% of the embryos. Nuclei without any dominant patch and similar to the pericentric-like pattern (see below) were found in 23% of the nuclei and 33% of the embryos. The remaining nuclei displayed the other patterns described at earlier stages. In contrast, the pericentric-like pattern was found in all embryos and 86% of the nuclei in the 8–16-

cell embryos, while the somatic-like female pattern was observed in less than 10% of the nuclei (Table 1 and the late 8-cell embryo in Fig. 4c, D).

To assess whether the somatic-like female profile was most likely associated with the Xi of the donor cell, bovine male SCNT embryos (N= 10) were also analyzed at the 1 to 8-cell stages. They never displayed the somatic-like female pattern (data not shown).

Nuclei of early 16–32-cell and morula female SCNT embryos displayed a pericentric-like profile and rarely (4–6%) the somatic-like female profile (Fig. 3a). While all nuclei of all IVF embryos examined displayed the well-contrasted pericentric pattern, 90% of the SCNT embryos displayed much more heterogeneity in the H3K27me3 staining profile than IVF embryos at these stages (Fig. 3a). Indeed, H3K27me3 staining displayed either very dense foci or hardly visible spots in most female SCNT embryos (Fig. 3a). Moreover, the difference between the IVF and SCNT embryos could be directly seen on mitotic figures at the early 16–32-cell stage (Fig. 2b), uncovering a different ratio of H3K27me3 labeling on pericentric heterochromatin and euchromatin and different staining intensity between chromosomes.

In mouse embryos obtained after fertilization, silencing of the paternal pericentric regions is transiently associated with enrichment in H3K27me3 catalyzed by PRC2 complexes [12]. The different ratios of H3K27me3 labeling between pericentric heterochromatin and euchromatin, which are observed at the 16–32-cell and morula stages in most SCNT bovine embryos as compared with IVF embryos, may therefore be due to an alteration in the silencing mechanisms. One possible mechanism supposes that H3K9me3 histones present in somatic pericentric heterochromatin are randomly replaced by other histones in a variable proportion of these regions following nuclear transfer, which leaves the possibility of PRC2 recruitment and subsequent H3K27me3 enrichment when these regions are silenced [12, 20]. Alternatively, the H3K27me3 enrichment that is observed in other than pericentric genomic regions in the nuclei of morula SCNT embryos may be associated with altered epigenetic regulation and gene expression.

However, at the blastocyst stage, all female SCNT embryos displayed the somatic-like female H3K27me3 profile in a significant proportion of trophoblast nuclei (10 to 38%), similar to IVF embryos (Fig. 3b). This pattern was never observed in male SCNT embryos (N=10), strongly suggesting that the somatic-like female profile was really associated with XCI. This will have to be confirmed by using other markers of XCI, such as the accumulation of *XIST* RNA on H3K27me3-enriched regions of the Xi [56] and monoallelic expression of X-linked genes [24, 57, 58].

In conclusion, our observations indicate that the H3K27me3-rich genomic regions are highly dynamic in bovine IVF embryos, as recently shown in mouse embryos [12]. Our results indicate a temporal correlation between EGA, i.e., the initiation of genome-wide transcription, and H3K27me3 remodeling and the end of partitioning of the parental genomes in early bovine IVF embryos. A similar correlation has been observed between EGA and the organization of chromosomal territories [59] and centromeric and pericentromeric regions [21] in the interphase nuclei of bovine embryos. The developmental dynamics of H3K27me3 give rise first to an embryo-specific, sex-independent, pericentric profile

that culminates immediately after the EGA stage. It corresponds to the transient enrichment in H3K27me3 in pericentric heterochromatin regions, as demonstrated recently in mouse embryos [12]. Two other profiles are then observed at the blastocyst stage in bovine embryos, which depend on sex: (i) a ‘male’ somatic-like profile, most likely corresponding to euchromatic labeling, and (ii) a somatic-like female profile in female embryos only, which is associated with the presence of the Xi-like H3K27me3-rich patch. This latter observation confirms that in cultured bovine embryos, XCI-related events are detected early [60]. Notably, *XIST* gene expression dramatically increases from at least the 8–16-cell stage onward [60].

Following SCNT, epigenetic regulation in the early bovine embryo appears to be flexible. In contrast to mouse SCNT embryos [28], the H3K27me3 epigenetic profile of the somatic donor nucleus is in bovine SCNT embryos largely remodeled. However, up to the 8-cell stage, the somatic-like female H3K27me3 profile was observed in a large proportion of the nuclei and embryos. The 8–16-cell stage marks the onset of a second phase of epigenetic changes, characterized by profiles resembling the pericentric profile to varying degrees. It does not preclude that the Xi of the donor cell remains partially enriched in H3K27me3, but it strongly suggests that in SCNT bovine embryos, large-scale H3K27me3 remodeling can occur several cell cycles after nuclear transfer and that EGA marks a key stage in remodeling this histone modification.

Recent studies have demonstrated that the local enrichment of histone modifications associated with inducible gene activity is controlled by transcription elongation in mammalian cells [6]. The temporal correlation of the changes in nuclear organization and chromatin structure ([15, 59], this paper) with EGA in early bovine embryos may therefore indicate that these changes depend somehow on genome-wide transcription. X chromosomes are a useful asset for understanding the role of EGA in chromatin remodeling in SCNT embryos. In normal female mouse embryos, transient transcription on both X chromosomes is clearly established [24, 57, 58]. On the other hand, different patterns of transcriptional activation on the Xi (and the *Xist* gene on the Xa) have been described in mouse SCNT embryos [28, 30, 61]. Consequently, it will be necessary in the future to determine whether the different pattern of H3K27me3 remodeling observed in mouse [28] and bovine (this study) SCNT embryos is correlated with a different pattern of chromosome-wide transcriptional activation of the Xi of the donor cell after nuclear transfer.

Acknowledgments

We are grateful to R Fleurot and P Adenot for their help and the use of the INRA-Jouy MIMA2 confocal facility, to Y Heyman for the IVM/IVF facility, to the staff of the INRA Experimental Station in Bressonsvilliers for helping with oocyte collection and to S Peron and P Bodinier for the preparation of cells. We thank two anonymous reviewers for their helpful criticisms. This work was supported by INRA. A Breton was the recipient of a PhD fellowship from the Ministère délégué à l’Enseignement Supérieur et à la Recherche, France.

References

- Yang X, Smith SL, Tian XC, Lewin HA, Renard JP, Wakayama T. Nuclear reprogramming of cloned embryos and its implications for therapeutic cloning. *Nat Genet* 2007; 39: 295–302.
- Bird A. Perceptions of epigenetics. *Nature* 2007; 447: 396–398.
- Jaenisch R, Bird A. Epigenetic regulation of gene expression: how the genome integrates intrinsic and environmental signals. *Nat Genet* 2003; 33 (Suppl): 245–254.
- Jenuwein T, Allis CD. Translating the histone code. *Science* 2001; 293: 1074–1080.
- Miao F, Natarajan R. Mapping global histone methylation patterns in the coding regions of human genes. *Mol Cell Biol* 2005; 25: 4650–4661.
- Rybtsova N, Leimgruber E, Seguin-Estevez Q, Dunand-Sauthier I, Krawczyk M, Reith W. Transcription-coupled deposition of histone modifications during MHC class II gene activation. *Nucleic Acids Res* 2007; 35: 3431–3441.
- Shao GB, Ding HM, Gong AH, Xiao DS. Inheritance of histone H3 methylation in reprogramming of somatic nuclei following nuclear transfer. *J Reprod Dev* 2008; 54: 233–238.
- Li E. Chromatin modification and epigenetic reprogramming in mammalian development. *Nat Rev Genet* 2002; 3: 662–673.
- Chavatte-Palmer P, Remy D, Cordonnier N, Richard C, Issenman H, Laigre P, Heyman Y, Mialot JP. Health status of cloned cattle at different ages. *Cloning Stem Cells* 2004; 6: 94–100.
- Chavatte-Palmer P, Heyman Y, Richard C, Monget P, LeBourhis D, Kann G, Chilliard Y, Vignon X, Renard JP. Clinical, hormonal, and hematologic characteristics of bovine calves derived from nuclei from somatic cells. *Biol Reprod* 2002; 66: 1596–1603.
- Farin PW, Piedrahita JA, Farin CE. Errors in development of fetuses and placentas from *in vitro*-produced bovine embryos. *Theriogenology* 2006; 65: 178–191.
- Puschendorf M, Terranova R, Boutsma E, Mao X, Isono K, Brykczynska U, Kolb C, Otte AP, Koseki H, Orkin SH, van Lohuizen M, Peters AH. PRC1 and Suv39h specify parental asymmetry at constitutive heterochromatin in early mouse embryos. *Nat Genet* 2008; 40: 411–420.
- Boyer LA, Plath K, Zeitlinger J, Brambrink T, Medeiros LA, Lee TI, Levine SS, Wernig M, Tajonar A, Ray MK, Bell GW, Otte AP, Vidal M, Gifford DK, Young RA, Jaenisch R. Polycomb complexes repress developmental regulators in murine embryonic stem cells. *Nature* 2006; 441: 349–353.
- Lee TI, Jenner RG, Boyer LA, Guenther MG, Levine SS, Kumar RM, Chevalier B, Johnstone SE, Cole MF, Isono K, Koseki H, Fuchikami T, Abe K, Murray HL, Zucker JP, Yuan B, Bell GW, Herbolsheimer E, Hannett NM, Sun K, Odom DT, Otte AP, Volkert TL, Bartel DP, Melton DA, Gifford DK, Jaenisch R, Young RA. Control of developmental regulators by Polycomb in human embryonic stem cells. *Cell* 2006; 125: 301–313.
- Martin C, Beaujean N, Brochard V, Audouard C, Zink D, Debey P. Genome restructuring in mouse embryos during reprogramming and early development. *Dev Biol* 2006; 292: 317–332.
- Payer B, Lee JT. X chromosome dosage compensation: how mammals keep the balance. *Annu Rev Genet* 2008; 42: 733–772.
- Kuzmichev A, Nishioka K, Erdjument-Bromage H, Tempst P, Reinberg D. Histone methyltransferase activity associated with a human multiprotein complex containing the enhancer of Zeste protein. *Genes Dev* 2002; 16: 2893–2905.
- Schuettengruber B, Chourrout D, Vervoort M, Leblanc B, Cavalli G. Genome regulation by polycomb and trithorax proteins. *Cell* 2007; 128: 735–745.
- Schoeftner S, Sengupta AK, Kubicek S, Mechtler K, Spahn L, Koseki H, Jenuwein T, Wutz A. Recruitment of PRC1 function at the initiation of X inactivation independent of PRC2 and silencing. *Embo J* 2006; 25: 3110–3122.
- Peters AH, Kubicek S, Mechtler K, O'Sullivan RJ, Derijck AA, Perez-Burgos L, Kohlmaier A, Opravil S, Tachibana M, Shinkai Y, Martens JH, Jenuwein T. Partitioning and plasticity of repressive histone methylation states in mammalian chromatin. *Mol Cell* 2003; 12: 1577–1589.
- Martin C, Brochard V, Migne C, Zink D, Debey P, Beaujean N. Architectural reorganization of the nuclei upon transfer into oocytes accompanies genome reprogramming. *Mol Reprod Dev* 2006; 73: 1102–1111.
- Maalouf WE, Liu Z, Brochard V, Renard JP, Debey P, Beaujean N, Zink D. Trichostatin A treatment of cloned mouse embryos improves constitutive heterochromatin remodeling as well as developmental potential to term. *BMC Dev Biol* 2009; 9: 11.
- Plath K, Fang J, Mlynarczyk-Evans SK, Cao R, Worringer KA, Wang H, de la Cruz CC, Otte AP, Panning B, Zhang Y. Role of histone H3 lysine 27 methylation in X inactivation. *Science* 2003; 300: 131–135.
- Okamoto I, Heard E. The dynamics of imprinted X inactivation during preimplantation development in mice. *Cytogenet Genome Res* 2006; 113: 318–324.
- Plath K, Talbot D, Hamer KM, Otte AP, Yang TP, Jaenisch R, Panning B. Developmentally regulated alterations in Polycomb repressive complex 1 proteins on the inactive X chromosome. *J Cell Biol* 2004; 167: 1025–1035.
- Kalantry S, Mills KC, Yee D, Otte AP, Panning B, Magnuson T. The Polycomb group protein Eed protects the inactive X-chromosome from differentiation-induced reactivation. *Nat Cell Biol* 2006; 8: 195–202.
- Wang J, Mager J, Chen Y, Schneider E, Cross JC, Nagy A, Magnuson T. Imprinted X inactivation maintained by a mouse Polycomb group gene. *Nat Genet* 2001; 28: 371–375.
- Bao S, Miyoshi N, Okamoto I, Jenuwein T, Heard E, Azim Surani M. Initiation of epigenetic reprogramming of the X chromosome in somatic nuclei transplanted to a mouse oocyte. *EMBO Rep* 2005; 6: 748–754.
- Chadwick BP. Variation in Xi chromatin organization and correlation of the H3K27me3 chromatin territories to transcribed sequences by microarray analysis. *Chromosoma* 2007; 116: 147–157.
- Nolen LD, Gao S, Han Z, Mann MR, Gie Chung Y, Otte AP, Bartolomei MS, Latham KE. X chromosome reactivation and regulation in cloned embryos. *Dev Biol* 2005; 279: 525–540.
- Memili E, First NL. Zygotic and embryonic gene expression in cow: a review of timing and mechanisms of early gene expression as compared with other species. *Zygote* 2000; 8: 87–96.
- Minami N, Suzuki T, Tsukamoto S. Zygotic gene activation and maternal factors in mammals. *J Reprod Dev* 2007; 53: 707–715.
- De La Fuente R, Hahnel A, Basrur PK, King WA. X inactive-specific transcript (Xist) expression and X chromosome inactivation in the preattachment bovine embryo. *Biol Reprod* 1999; 60: 769–775.
- Pichugin A, Le Bourhis D, Adenot P, Lehmann G, Audouard C, Renard JP, Vignon X, Beaujean N. Dynamics of constitutive heterochromatin: two contrasted kinetics of genome restructuring in early cloned bovine embryos. *Reproduction* 2010; 139: 129–137.
- Bourchis D, Le Bourhis D, Patin D, Niveleau A, Comizzoli P, Renard JP, Viegas-Pequignot E. Delayed and incomplete reprogramming of chromosome methylation patterns in bovine cloned embryos. *Curr Biol* 2001; 11: 1542–1546.
- Dean W, Santos F, Stojkovic M, Zakhartchenko V, Walter J, Wolf E, Reik W. Conservation of methylation reprogramming in mammalian development: aberrant reprogramming in cloned embryos. *Proc Natl Acad Sci USA* 2001; 98: 13734–13738.
- Kang YK, Park JS, Koo DB, Choi YH, Kim SU, Lee KK, Han YM. Limited demethylation leaves mosaic-type methylation states in cloned bovine pre-implantation embryos. *Embo J* 2002; 21: 1092–1100.
- Kremenskoy M, Kremenska Y, Suzuki M, Imai K, Takahashi S, Hashizume K, Yagi S, Shiota K. DNA methylation profiles of donor nuclei cells and tissues of cloned bovine fetuses. *J Reprod Dev* 2006; 52: 259–266.
- Liu J, Liang X, Zhu J, Wei L, Hou Y, Chen DY, Sun QY. Aberrant DNA methylation in 5' regions of DNA methyltransferase genes in aborted bovine clones. *J Genet Genomics* 2008; 35: 559–568.
- Liu JH, Yin S, Xiong B, Hou Y, Chen DY, Sun QY. Aberrant DNA methylation imprints in aborted bovine clones. *Mol Reprod Dev* 2008; 75: 598–607.
- Li S, Li Y, Du W, Zhang L, Yu S, Dai Y, Zhao C, Li N. Aberrant gene expression in organs of bovine clones that die within two days after birth. *Biol Reprod* 2005; 72: 258–265.
- Yang L, Chavatte-Palmer P, Kubota C, O'Neill M, Hoagland T, Renard JP, Taneja M, Yang X, Tian XC. Expression of imprinted genes is aberrant in deceased newborn cloned calves and relatively normal in surviving adult clones. *Mol Reprod Dev* 2005; 71: 431–438.
- Santos F, Zakhartchenko V, Stojkovic M, Peters A, Jenuwein T, Wolf E, Reik W, Dean W. Epigenetic marking correlates with developmental potential in cloned bovine preimplantation embryos. *Curr Biol* 2003; 13: 1116–1121.
- Renard JP, Maruotti J, Jouneau A, Vignon X. Nuclear reprogramming and pluripotency of embryonic cells: Application to the isolation of embryonic stem cells in farm animals. *Theriogenology* 2007; 68 (Suppl 1): S196–205.
- Gall L, Le Bourhis D, Ruffini S, Boulesteix C, Vignon X. Unexpected nuclear localization of Cdc25C in bovine oocytes, early embryos, and nuclear-transferred embryos. *Reproduction* 2008; 135: 431–438.
- Menezes Y, Gerard M, Thibault C. Culture of the bovine graafian follicle in a continuous liquid and gas flow system. *CR Acad Sci Hebd Seances Acad Sci D* 1976; 283: 1309–1311 (In French).
- Ross PJ, Ragina NP, Rodriguez RM, Iager AE, Siripattarapravat K, Lopez-Corrales N, Cibelli JB. Polycomb gene expression and histone H3 lysine 27 trimethylation changes during bovine preimplantation development. *Reproduction* 2008; 136: 777–785.
- Santos F, Peters AH, Otte AP, Reik W, Dean W. Dynamic chromatin modifications characterise the first cell cycle in mouse embryos. *Dev Biol* 2005; 280: 225–236.
- Cowell IG, Aucott R, Mahadevaiah SK, Burgoyne PS, Huskisson N, Bongiorno S, Prantera G, Fanti L, Pimpinelli S, Wu R, Gilbert DM, Shi W, Fundele R, Morrison

- H, Jeppesen P, Singh PB. Heterochromatin, HP1 and methylation at lysine 9 of histone H3 in animals. *Chromosoma* 2002; 111: 22–36.
50. Mayer W, Smith A, Fundele R, Haaf T. Spatial separation of parental genomes in preimplantation mouse embryos. *J Cell Biol* 2000; 148: 629–634.
51. Park KE, Magnani L, Cabot RA. Differential remodeling of mono- and trimethylated H3K27 during porcine embryo development. *Mol Reprod Dev* 2009; 76: 1033–1042.
52. Kirszenbaum M, Cotinot C, Leonard M, Vaiman M, Fellous M. Diagnosis of the sex of bovine embryos using molecular biology. *Reprod Nutr Dev* 1990; (Suppl 1): 125s–132s.
53. Tominaga K, Hamada Y. Efficient production of sex-identified and cryosurvived bovine *in-vitro* produced blastocysts. *Theriogenology* 2004; 61: 1181–1191.
54. Perche PY, Vourc'h C, Konecny L, Souchier C, Robert-Nicoud M, Dimitrov S, Khochbin S. Higher concentrations of histone macroH2A in the Barr body are correlated with higher nucleosome density. *Curr Biol* 2000; 10: 1531–1534.
55. Coppola G, Pinton A, Joudrey EM, Basrur PK, King WA. Spatial distribution of histone isoforms on the bovine active and inactive X chromosomes. *Sex Dev* 2008; 2: 12–23.
56. Chadwick BP, Willard HF. Multiple spatially distinct types of facultative heterochromatin on the human inactive X chromosome. *Proc Natl Acad Sci USA* 2004; 101: 17450–17455.
57. Huynh KD, Lee JT. Inheritance of a pre-inactivated paternal X chromosome in early mouse embryos. *Nature* 2003; 426: 857–862.
58. Okamoto I, Otte AP, Allis CD, Reinberg D, Heard E. Epigenetic dynamics of imprinted X inactivation during early mouse development. *Science* 2004; 303: 644–649.
59. Koehler D, Zakhartchenko V, Froenicke L, Stone G, Stanyon R, Wolf E, Cremer T, Brero A. Changes of higher order chromatin arrangements during major genome activation in bovine preimplantation embryos. *Exp Cell Res* 2009; 315: 2053–2063.
60. Nino-Soto MI, Basrur PK, King WA. Impact of *in vitro* production techniques on the expression of X-linked genes in bovine (*bos taurus*) oocytes and pre-attachment embryos. *Mol Reprod Dev* 2007; 74: 144–153.
61. Eggan K, Akutsu H, Hochedlinger K, Rideout W, 3rd, Yanagimachi R, Jaenisch R. X-chromosome inactivation in cloned mouse embryos. *Science* 2000; 290: 1578–1581.